J. Fluid Mech. (2002), *vol.* 466, *pp.* 149–177. © 2002 Cambridge University Press
DOI: 10.1017/S0022112002001222 Printed in the United Kingdom

The weakly nonlinear interfacial stability of a core–annular flow in a corrugated tube

By HSIEN-HUNG WEI AND DAVID S. RUMSCHITZKI

Department of Chemical Engineering, City College of New York,
New York, NY10031, USA
and Graduate School and University Center CUNY, New York, NY 10016, USA

(Received 2 April 2001 and in revised form 23 January 2002)

A core–annular flow, the concurrent axial flow of two immiscible fluids in a circular tube or pore with one fluid in the core and the other in the wetting annular region, is frequently used to model technologically important flows, e.g. in liquid–liquid displacements in secondary oil recovery. Most of the existing literature assumes that the pores in which such flows occur are uniform circular cylinders, and examine the interfacial stability of such systems as a function of fluid and interfacial properties. Since real rock pores possess a more complex geometry, the companion paper examined the linear stability of core–annular flows in axisymmetric, corrugated pores in the limit of asymptotically weak corrugation. It found that short-wave disturbances that were stable in straight tubes could couple to the wall's periodicity to excite unstable long waves. In this paper, we follow the evolution of the axisymmetric, linearly unstable waves for fluids of equal densities in a corrugated tube into the weakly nonlinear regime. Here, we ask whether this continual generation of new disturbances by the coupling to the wall's periodicity can overcome the nonlinear saturation mechanism that relies on the nonlinear (kinematic-condition-derived) wave steepening of the Kuramoto–Sivashinsky (KS) equation. If it cannot, and the unstable waves still saturate, then do these additional excited waves make the KS solutions more likely to be chaotic, or does the dispersion introduced into the growth rate correction by capillarity serve to regularize otherwise chaotic motions?

We find that in the usual strong surface tension limit, the saturation mechanism of the KS mechanism remains able to saturate all disturbances. Moreover, an additional capillary-derived nonlinear term seems to favour regular travelling waves over chaos, and corrugation adds a temporal periodicity to the waves associated with their periodical traversing of the wall's crests and troughs. For even larger surface tensions, capillarity dominates over convection and a weakly nonlinear version of Hammond's no-flow equation results; this equation, with or without corrugation, suggests further growth. Finally, for a weaker surface tension, the leading-order base flow interface follows the wall's shape. The corrugation-derived excited waves appear able to push an otherwise regular travelling wave solution to KS to become chaotic, whereas its dispersive properties in this limit seem insufficiently strong to regularize chaotic motions.

1. Introduction

Core–annular flows (CAFs), the two-phase flow configuration where one fluid occupies a cylindrical region, surrounded by an annulus of a second fluid, which is

immiscible with the first, have recently been used as model systems for improving many technologies such as liquid–liquid displacements in secondary oil recovery (Slattery 1974) and understanding respiratory distress in the lung, including surfactant transport (Johnson *et al.* 1991; Halpern & Grotberg 1993; Otis *et al.* 1993). In secondary oil recovery, typically an aqueous phase of low tension with water is introduced to displace oil lodged in rock pores. The displacement takes the form of a winding train of long slugs of the non-wetting fluid separated by pools of the wetting fluid and riding over a thin cushion of the wetting fluid. The rock determines which fluid is more wetting. In either case the train velocities are slow enough that the capillary number (the product of the slug velocity and the wetting layer viscosity divided by the interfacial tension) and the Reynolds number (base on either phase) are much less than one. For such cases the asymptotic theory of Bretherton (1961) predicts a ratio of wetting-layer thickness to pore radius proportional to $Ca^{2/3}$. Far from the edge of the slug, the flow resembles a core–annular flow. Should instabilities cause the film to rupture, thereby bringing the non-wetting fluid in contact with the wall, slow or inhibited respreading of the wetting layer can significantly inhibit the overall train mobility.

Many premature babies as well as adults afflicted by diseases such as adult respiratory distress syndrome lack a functioning surfactant normally produced by alveolar type II epithelial cells (Kamm & Schroter 1989; Otis *et al.* 1993); this condition leads to impaired breathing. Lung bronchioli are tubelike structures that branch out into many generations, and this array of vastly different sized tubes expands and contracts during breathing. A thin layer of fluid (varying from water to mucus) coats the inside of these tubes. In the absence of effective surfactants, either the tube walls themselves can collapse or a hydrodynamic instability can transform the fluid layer into a lens which can block the flow of air and decrease the effective lung volume. Such collapse appears to take place first in the terminal (small) bronchioles during exhalation (Johnson *et al.* 1991). Breathing induces very slow flow in this layer, and the system resembles a gas-core core–annular flow. Since even a slow viscous flow can compete with surface tension to determine the system's stability (Papageorgiou, Maldarelli & Rumschitzki 1990; Georgiou *et al.* 1992), this problem is a subject of interest.

A perfect (the cylinder and the annulus are coaxial) core–annular flow (PCAF) in a straight, circular tube of uniform cross-section is often adopted as an ideal model on which most studies are based. Understanding the mechanism of instability in this system is important because we may want to encourage or discourage instability depending on the application. The linear stability, for both the case with and without a base flow, is characterized by capillarity, viscosity stratification and density stratification. Infinitesimal disturbances arise at the fluid–fluid interface and they may grow or be damped. Capillarity, which stabilizes short waves and destabilizes long waves, generally plays the most decisive role in determining the interfacial stability in the cylindrical geometry and in particular in the CAF. A whole literature (see § 2) has led to a detailed understanding of how fluid and interfacial properties affect the system's linear and nonlinear stability in the PCAF configuration, particularly in the strong-surface-tension regime.

However, in applications such as liquid–liquid displacements in rock pores or lung respiration the assumption of uniform tube radius is inappropriate, and it is worth examining whether the coupling of this geometric factor is (at least) as important as the other effects already considered. In the companion paper (Wei & Rumschitzki 2002, hereinafter referred to as WR), we develop an asymptotic theory for the effect of a slight corrugation on the (base flow and the) linear stability

of a CAF and find that the coupling of short-wave interfacial disturbances to the pore wall's corrugation harmonics excites unstable long waves. Yet in PCAF theory, weakly nonlinear contributions steepen, and thereby shorten, linearly growing long waves, resulting in their stabilization due to capillarity. The goal of this paper is to examine these opposing trends in the weakly nonlinear regime of a slightly corrugated CAF. We begin with a brief literature review, followed by problem formulation and scalings, leading to the equation governing the system's weakly nonlinear evolution for a particular parameter regime. Numerical solution of this equation and discussion of the results then precede a brief summary.

2. Literature and motivation

As noted, capillarity is generally the most important factor in the cylindrical geometry. Capillarity acts in two ways: it destabilizes the interfacial circumferential curvature and stabilizes the longitudinal curvature of an interfacial deflection. The result of this competition is that disturbances with wavelengths shorter than the undisturbed interfacial circumference are linearly stable and those longer are linearly unstable owing to capillarity. In the presence of a base flow in a PCAF, capillarity and viscosity (and density in the vertical arrangement) stratification compete, and Joseph and coworkers (Hu & Joseph 1989; Preziosi, Chen & Joseph 1989; Chen, Bai & Joseph 1990) have performed extensive investigations of CAFs by numerically solving the Orr–Sommerfeld equation. They have found for the parameter regime characteristic of lubricated pipelining (Preziosi *et al.* 1989) that viscosity stratification can stabilize the long-wave destabilization of capillarity at large enough, but not too large, Reynolds numbers. There exists a window of stability in Reynolds number space in which the CAF is linearly stable. For most applications of interest, the thickness of the annular fluid is much smaller than the tube radius. As such, Georgiou *et al.* (1992) have developed thin-film asymptotics (in the small ratio ε of the undisturbed annulus thickness to core radius) to examine analytically the linear stability of a PCAF in a vertical arrangement. With axisymmetric disturbances whose wavelengths are comparable to the tube circumference, they have shown analytically that viscosity stratification can stabilize the capillary instability for the ratio $m < 1$ of annulus-to-core fluid viscosities, whereas it is destabilizing for $m > 1$.

Study of the nonlinear stability regime of these thin-film systems is important for a better understanding of the system's response to disturbances of finite magnitude as well as to investigate the fate of linearly unstable waves. Hammond (1985) studied the two-fluid CAF in a tube with a thin annular film is the absence of a base flow, for which the core dynamics become irrelevant at leading order in the ratio ε of the film thickness to the undisturbed core radius. His nonlinear analysis showed that long-wave disturbances can grow nonlinearly and this suggests that they could potentially lead to film breakup into lenses when sufficient liquid is present. However, the extent of the validity of his equation was limited by the thin-film approximation, which particularly impacts the mean curvature of the interface. This $O(\varepsilon)$ approximation admits a collar volume that never goes through a maximum so that the collar is always stable and need not form a lens. Gauglitz & Radke (1988) extended Hammond's analysis in an *ad hoc* manner equivalent to a first-order Padé, rather than a Taylor, approximation by keeping the full nonlinear circumferential curvature in the capillary but linearizing everything else in the normal stress balance at the fluid–fluid interface. Their analysis can predict the transition from collars to lenses, whereas Hammond's thin-film analysis might be able to predict this transition only at a higher order in ε approximation.

In the presence of a base flow and very strong surface tension, Frenkel *et al.* (1987) found that the Kuramoto–Sivashinky (KS) equation governs the weakly nonlinear evolution of fluids with matched viscosities and densities. In their case, only capillarity destabilizes and the dynamics of the core slave those of the film. The nonlinear coupling to the base flow through the kinematic condition can steepen unstable interfacial long waves. This gives rise to shorter length scales which become stabilized by the longitudinal component (the fourth derivative of the interfacial deflection) of the interfacial tension force. The KS equation has arisen in a variety of applications and exhibits complex dynamic behaviours depending on the period length. Numerical solutions on a periodic domain have exhibited non-trivial steady states (Chang 1987), travelling waves (Hooper & Grimshaw 1985), and spatial and temporal chaotic motions (Sivashinky & Michelson 1980; Hyman & Nicolaenko 1986; Hyman, Nicolaenko & Zaleski 1986). The most important feature of these investigations is that KS seems to yield smooth and bounded solutions.

Papageorgiou *et al.* (1990) systematically developed a weakly nonlinear analysis of CAF film flows for generally different viscosities and densities and for surface tensions where the core dynamics are integrally coupled to the interfacial evolution. They derived an amplitude equation to describe the interfacial dynamics which turns out to be a KS equation modified by the inclusion of additional terms containing integral kernels involving core quantities. In the case of slow and moderate flows, this equation has non-local terms that reflect the coupling due to viscosity stratification of the dynamics of the core to the interfacial evolution. These core-coupling terms also give rise to additional dispersive and dissipative effects. They can lead to either chaotic interfacial motions for weak dispersion, or more typically to nonlinear travelling waves having more than one length scale for strong dispersion. These additional terms demonstrate the regularizing effect of dispersion. This complements and is consistent with the model results obtained by Kawahara (1983) and Kawahara & Toh (1988) who added a simple third derivative dispersion term to the KS equation and found regularization.

The point here is that, apparently, the KS-like systems can saturate the linearly unstable waves in the weakly nonlinear regime. Kerchman (1995) allows the interfacial disturbances to grow to sizes comparable to the film thickness, but instead requires negligible interfacial shear, to examine strongly nonlinear interfacial dynamics of a CAF. His analysis includes the weakly nonlinear analysis as special case. KS-type saturation of the instability occurs for sufficiently small $\varepsilon^2 J/Re_1$ (where $Re_1/J = \mu_1 W_0/\gamma$, μ_1 being the core viscosity, W_0 the centreline base flow velocity and γ the interfacial tension, can be regarded as the capillary number based on the core fluid). When $\varepsilon^2 J/Re_1$ is sufficiently large, though, the core–annular arrangement may collapse because the interface can strongly bulge into the core as a result of strong capillary forces acting in the neighbourhood of an interfacial trough. As such, the interfacial stability of a PCAF in a circular tube is fairly well understood.

As noted, in real core–annular flow systems such as occur in secondary oil recovery, two fluids flow through uneven channels in the porous rock, and thus do not posses an ideal geometry as do flows in a perfectly cylindrical tube. Similarly, the extensive branching of the bronchiole system represents a system with a frequently changing cross-section. It is thus conceivable that pore corrugations may play a role in determining the stability of the system that is at least as important as the effects already considered. However, there are good reasons why we might neglect them in the first analysis. Let us consider briefly how pore corrugations complicate the problem. First, such non-ideality will cause the base state to be significantly changed.

Even the axisymmetric base flow pattern in a tube of varying cross-section will be two dimensional, rather than just a purely axial velocity as a function of only the radial position. This deviation from parallel flow can interact strongly with the disturbance introduced in the stability analysis. For instance, consider the flow of a single fluid in a tube of sinusoidally varying cross-section, even for small Reynolds number Re. Inertial effects can be significant when the axial variation of the tube radius $\mathrm{d}R/\mathrm{d}z$ is as rapid as $O(1/Re)$. Moreover, it is unlikely that we would be able to solve for the base state exactly in closed form. Cylindrical tube theory clearly does not include these effects. To access them, it is necessary to extend the scope of this theory to include the varying geometry.

There have been several studies of base flows without an accompanying stability analysis. Wang (1981) considered a film flowing slowly down a wavy inclined plate, where the striations are parallel to the overall flow. He applied a perturbation method with respect to the small amplitude of the corrugation. He found that for a fixed mean film depth, the flow transverse to the striations is decreased relative to that of a smooth plate while the flow along the striations is increased. Dassori, Deiber & Cassano (1984) analysed a two-fluid system in a symmetric sinusoidally varying two-dimensional channel. They focused only on the case of an outer fluid (e.g. a gas) with very low density and viscosity ratios relative to the core fluid. They found that the fluid interface exhibited a wavy shape, characterized by an amplitude and a phase shift, relative to the channel, which are functions of surface tension, density and viscosity ratios, flow rate, and the wavenumber of the wall. Recently, Kang & Chen (1995) extended Wang's analysis to the case with two fluid–fluid interfaces in a planar system and a similar picture resulted. In cases of large variation due to corrugation, perturbation techniques as above are no longer applied. Pozrikidis (1988) extends Wang's problem to large corrugations and solves the two-dimensional creeping flow numerically on a periodic domain by using the boundary-integral method. He shows that Wang's asymptotic analysis overestimates the effect of the wall's waviness on the deflection of the interface, particularly at high flow rates.

However, linear or nonlinear stability issues associated with flows in the corrugated configuration, especially interfacial problems, have only been explored in a preliminary manner. In the case of no flow, Gauglitz & Radke (1990) employed their previous analysis (1988) to examine how constrictions affect foam formation in gas–liquid displacements for the case where the radius varies slowly in the axial direction. They showed that the time required to snap a collar off strongly depends on the neck radius of the constriction and that the length of the constriction is not crucial to the instability. A similar conclusion was also drawn by Ransokoff, Gauglitz & Radke (1987) and Ratulowski & Chang (1989), who analysed the case where constrictions have various cross-sections.

Tougou (1978) investigated the linear and weakly nonlinear stability of a viscous film flowing down an inclined uneven wall in the presence of surface tension. In the leading order of a shallow thickness parameter ε, defined here as the ratio of the mean film thickness to the wavelength of the wall, the linear stability of the base flow is identical to that for the plane wall case. His weakly nonlinear analysis derived a KS-type equation incorporating the non-uniformity of the wall and showed that the long-time interfacial evolution for an asymptotically long-wave wall is no longer spatially periodic owing to the non-parallel base flow.

In WR (see also Wei & Rumschitzki 2000), we have developed an analysis that uses asymptotic methods and Floquet–Bloch theory to analytically examine the lin-

ear stability of a CAF in a corrugated tube. We develop steady base flows in an asymptotic sense in powers of the small parameters ε and σ, the latter characterizing the strength of the corrugation relative to the mean annulus thickness. We then derive the corresponding linear stability to the leading order in both small parameters. (All discussions below of this problem's base flow and linear stability results implicitly refer to WR.) This procedure yields a linear interfacial evolution equation with non-constant coefficients. Floquet–Bloch theory leads to the eigenvalue spectra that depend on the wall's wavenumber k and these spectra exhibit periodicity in α-space, where α is the wavenumber of the initial disturbance. Direct numerical solutions of the partial differential equation that governs the interfacial evolution for a variety of initial conditions are performed and compare very well with the eigenvalue spectra. The results reveal that the wavelength of the initial interfacial disturbance is modified owing to interactions with the wall's corrugation. As a result, in contrast to the case of a CAF in straight tube, an initial disturbances whose wavelength is shorter than the circumference of the undisturbed fluid–fluid interface can also lead to an instability owing to the unstable higher wall corrugation harmonics excited by the initial disturbance.

This discussion suggests two opposing trends in the weakly nonlinear regime of a core–annular flow in a tube of varying cross-section. On the one hand, coupling of an initially short wavelength disturbance to the wall's corrugation excites unstable long wavelength wall harmonics of the initial disturbance. On the other hand, the nonlinearity in KS and related equations steepen growing long waves, thereby shortening their effective wavelength and stabilizing them via the fourth derivative capillary term. Our aim in this paper is to systematically extend our previous analysis into the weakly nonlinear regime in order to examine the interaction of these two trends. In particular, can the nonlinearity saturate all of the unstable harmonics generated by the corrugation and will the resulting dynamics be chaotic or regular?

3. Mathematical formulation

3.1. *Governing equations and boundary conditions*

Two immiscible, viscous, incompressible fluids are flowing axisymmetrically in a core–annular arrangement in a horizontal tube of radius $R_2(z)$ that varies in the axial direction with slight corrugation (see figure 1). The interface is given by $r = S(z,t)$. The core region, defined by $0 \leqslant r \leqslant S(z,t)$, is occupied by fluid 1 and the annulus, $S(z,t) \leqslant r \leqslant R_2(z)$, is filled by fluid 2. Since the flow fields are assumed to be axisymmetric, they only have velocity components $(u, 0, w)$ in terms of the cylindrical polar coordinates (r, θ, z). We non-dimensionalize the velocity, pressure, length scales and time with the characteristic quantities W_0, ρW_0^2, R_0 and R_0/W_0, respectively. R_0 is the mean core radius; W_0 is the axial velocity at the central line $r = 0$ (note: application to the respiratory problem having a gas core requires a rescaling with γ/μ where γ is the surface tension, rather than the centreline velocity) in the uncorrugated base flow with inner and outer radii R_0 and the mean value of R_2, respectively; and ρ is the density of the fluids taken for now to be equal (since the effects of density differences tend to be of higher order than viscosity differences or surface tension (Georgiou *et al.* 1992)).

The non-dimensional governing equations in each phase are given by

$$w_t + uw_r + ww_z = -p_z + \frac{1}{Re_i}\nabla^2 w, \tag{3.1a}$$

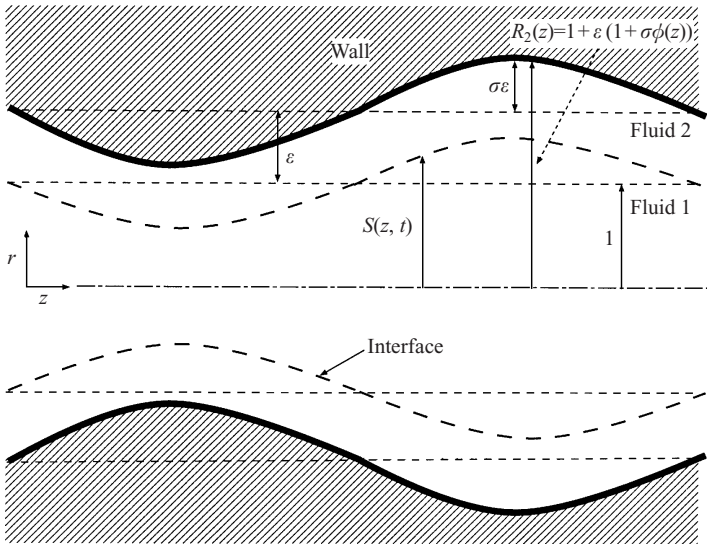

FIGURE 1. System diagram. Wall is $R_2(z) = 1 + \varepsilon(1 + \sigma\phi(z))$; interface is $S(z,t)$.

$$u_t + uu_r + wu_z = -p_r + \frac{1}{Re_i}\left(\nabla^2 u - \frac{u}{r^2}\right), \tag{3.1b}$$

$$\frac{1}{r}(ru)_r + w_z = 0, \tag{3.1c}$$

where

$$\nabla^2 = \frac{\partial^2}{\partial r^2} + \frac{1}{r}\frac{\partial}{\partial r} + \frac{\partial^2}{\partial z^2},$$

$i = 1, 2$ denotes the core and the annulus, respectively, subscripts denote partial derivatives and the Reynolds number is given by $Re_i = \rho W_0 R_0/\mu_i$. We use Re_1 for the core as the reference Reynolds number. The annulus Reynolds number is $Re_2 = Re_1/m$, in which $m = \mu_2/\mu_1$ is the viscosity ratio of the annulus to the core.

Define the jump notation $[\bullet] = (\bullet)_1 - (\bullet)_2$. The following boundary conditions are used. Velocities vanish on the wall $R_2(z)$:

$$w = 0, \quad u = 0 \quad \text{at} \quad r = R_2(z). \tag{3.2a}$$

The velocities are continuous across the interface,

$$[w] = 0, \quad [u] = 0, \quad \text{at} \quad r = S(z,t). \tag{3.2b}$$

The tangential stress and normal stress balances apply at the fluid–fluid interface:

$$\left[\frac{1}{Re}(u_z + w_r)(1 - S_z^2) + \frac{2}{Re}u_r S_z - \frac{2}{Re}w_z S_z\right] = 0 \quad \text{at} \quad r = S(z,t), \tag{3.2c}$$

$$-\left[p - \frac{2}{Re}u_r - \left(-p + \frac{2}{Re}w_z\right)S_z + \frac{2}{Re}(u_z + w_r)S_z\right]$$
$$= \frac{J}{Re_1^2}\left(S_{zz} - \frac{1}{S}(1 + S_z^2)\right)(1 + S_z^2)^{-3/2} \quad \text{at} \quad r = S(z,t), \tag{3.2d}$$

where $J = \gamma R_0 \rho/\mu_1^2$ is the surface tension parameter used by Chandrasekhar (1968)

and where γ is the interfacial tension. The kinematic condition, which determines the shapes of the interface, is

$$u = S_t + wS_z \quad \text{at} \quad r = S(z,t), \tag{3.2e}$$

Finally, the flow field of the core must be bounded at the central line, i.e.

$$w \text{ bounded and } u = 0 \text{ as } \quad r \to 0. \tag{3.2f}$$

3.2. *Scalings and asymptotic formulation*

In our study of the linear stability of the system, we assumed an asymptotically small wall corrugation $R_2(z) = 1 + \varepsilon(1 + \sigma\phi(z))$, where σ is a small parameter characterizing the size of the corrugation and $\phi(z)$ is an order one shape function. We found that the scaling relation $J/Re_1 \sim 1/\varepsilon^2$ yields a non-trivial corrugated base flow in the CAF configuration and we calculated it to leading order in ε and σ. The solution for the flow pattern is determined by the interfacial deflection $\eta(z)$ (the base state's interfacial position $S_b(z) = 1 + \sigma\varepsilon\eta(z) + \cdots$), which the following equation for the interfacial shape governs:

$$\frac{J_0}{3\lambda}(\eta_{zzz} + \eta_z) + 2\eta = 2\phi, \tag{3.3}$$

where $J = J_0/\varepsilon$ and $Re_1 = \lambda\varepsilon$, λ and J_0 are both order one constants. Note that the solution to η is independent of viscosity stratification (m) since the core does not contribute to leading order at these scales and $J_0/6\lambda$ is just the ratio of the capillary to the shear forces ($Re_1/J = Ca$, the capillary number). Introduce a stretched film variable $y := 1 - (r-1)/\varepsilon$. The film solution (double and single overbars denote PCAF and the corrugation's correction to the base flow, respectively) is

$$w_b = \bar{\bar{w}} + \bar{w} = \frac{2\varepsilon}{m}y + \varepsilon\sigma\left(\frac{J_0}{m\lambda}(\eta_{zzz} + \eta_z)(\tfrac{1}{2}y^2 - y) + \frac{2}{m}\phi\right) + O(\varepsilon^2, \varepsilon^2\sigma, \sigma^2\varepsilon), \tag{3.4a}$$

$$u_b = \bar{u} = \varepsilon^2\sigma\left(\frac{J_0}{m\lambda}(\eta_{zzzz} + \eta_{zz})(\tfrac{1}{6}y^3 - \tfrac{1}{2}y^2) + \frac{2}{m}\phi_z y\right) + O(\varepsilon^3\sigma, \sigma^2\varepsilon^2), \tag{3.4b}$$

$$p_b = \bar{\bar{p}} + \bar{p} = \bar{\bar{p}} + \frac{\sigma}{\varepsilon^2}(\eta + \eta_{zz}) + O\left(\frac{\sigma}{\varepsilon}, \frac{\sigma^2}{\varepsilon}\right). \tag{3.4c}$$

We do not quote the base flow of the core since it merely slaves the film (up to $O(1)$ Re_1) and does not contribute to the leading-order stability of the system. Also, WR extends the previous analysis to both $J_0/\lambda \gg 1$ and $\varepsilon \ll J_0/\lambda \ll 1$ regimes without significant change to the formulation.

With the asymptotic, steady base flows, we now begin the corresponding asymptotic weakly nonlinear stability analysis. Instead of an infinitesimal disturbance for the linear analysis, we introduce a finite axisymmetric disturbance of size δ at the steady interface in such a way that $S(z,t) = S_b(z) + \delta\xi(z,t)$, where $S_b(z)$ is the interface of the corrugated base state, $\xi(z,t)$ is an unknown order one function responsible for the disturbance, and δ is small compared with the undisturbed core radius and film thickness, i.e. $\delta \ll |S_b|,\ \varepsilon$. Clearly, $\delta \to 0$ recovers the base flows, and $O(\delta)$ leads to the linear stability problem. In general, the fully nonlinear analysis allows $\delta \sim \varepsilon$, which means that the size of the disturbance is comparable to the film thickness. We scale $\delta = \delta(\sigma, \varepsilon) \ll \varepsilon$ to constrain disturbances within the weakly nonlinear regime.

We first determine the scalings of the disturbed quantities before formulating the perturbation scheme. We follow the scaling procedure used in the linear analysis, which is similar to Hammond (1983), Papageorgiou *et al.* (1990) and Georgiou *et al.*

(1992). We use ε, the ratio of the mean undisturbed film thickness to the mean core radius as the small parameter. By substituting for r in terms of y we can make the thin film explicit, separate the film's radial scale from its axial scale and from both scales in the core. As such, radial derivatives in the film are large, i.e. $\partial/\partial r = -(1/\varepsilon)(\partial/\partial y)$. Let (w', u', p') and (W', U', P') represent the disturbed quantities for the film and the core, respectively. We can estimate the scalings of these quantities in the case of $Re_1 = \lambda\varepsilon$ and $J = J_0/\varepsilon$ by using the scaling relation for the base flows together with the governing equations and boundary conditions. From the normal stress condition, $p' \sim \delta/\varepsilon^3$. Relating w' with p' by use of the lubrication equations in the film brings out $w' \sim \delta$, and $u' \sim \varepsilon\delta$ follows by continuity. For the core, which lacks separable length scales, both W' and U' are of order δ, which is a consequence of the continuity of velocity, and P' is of order δ/ε from the equations of motion.

We now seek a consistent order for δ. Since the annular region is thin, the lubrication equations govern the flow there. The nonlinear inertia of the film is of higher order, and thus the nonlinear terms in the stability analysis derive from the kinematic condition. This condition couples the derivative of the disturbed interface position either to the base flow velocity at the disturbed interfacial position, or directly to the disturbed flows. Thus, the kinematic condition should provide the scaling of δ in this weakly nonlinear analysis. We begin with the expansions for the film,

$$w = w_b + \delta w', \quad u = u_b + \varepsilon\delta u', \quad p = p_b + \frac{\delta}{\varepsilon}p', \tag{3.5a–c}$$

and for the core,

$$W = W_b + \delta W', \quad U = U_b + \delta U', \quad P = P_b + \frac{\delta}{\varepsilon}P', \tag{3.5d–f}$$

where the quantities with subscript b denote the base flow quantities, which have non-trivial σ and ε expansions. Let $(w_b, u_b) = (\varepsilon\bar{w}_0 + \cdots, \sigma\varepsilon^2\bar{u}_0 + \cdots)$ for the film base flow. Then the kinematic condition, evaluated at the base interface $S_b(z) = 1 + \sigma\varepsilon\eta(z)$ (and not at $r = 1$), expanded with respect to δ, gives

$$\begin{aligned}\delta(-\sigma\varepsilon\bar{u}_{0y}\xi + \varepsilon u') - \delta^2 u'_y\xi + O(\sigma\delta^2) = \delta\xi_t + \varepsilon\delta\bar{w}_0\xi_z + \delta S_{bz}(-\bar{w}_{0y}\xi + w') \\ + \delta^2\xi_z(-\bar{w}_{0y}\xi + w') + O(\delta^3).\end{aligned} \tag{3.6}$$

Note that $S_{bz} \sim \sigma\varepsilon$ here. We introduce the long time scale $\tau = \varepsilon t$ to capture the dynamics of the leading order of (3.6) at $O(\varepsilon\delta)$. Since the weakly nonlinear analysis requires $\delta/\varepsilon \ll 1$, δ/ε should be scaled using the system's small parameters ε and σ. Different scaling choices for the parameters may lead to different dynamic characters. We shall discuss this in the next section.

Below we plug the appropriate asymptotic expansions into the governing equations and the boundary conditions, extract the corrugated base flow contribution and derive an equation that governs the stability of the system up to $O(\delta^2)$ within the weakly nonlinear regime. In order to allow a larger scope to this scaling analysis and to provide the context for a general discussion later on, it is more convenient to keep δ unscaled in (3.5) during the formulation.

A full knowledge of the base state to all orders in σ and ε provides an exact solution of the nonlinear, steady-state Navier–Stokes equations subject to the conditions of the corrugated boundary. In WR, we have only solved the base flow asymptotically and have thus far only determined its leading-order contributions explicitly. However, when substituting (3.5) into (3.1) and (3.2), we shall use the fact that the full steady-state solution satisfies the steady-state equations and boundary conditions exactly and

its truncated solutions satisfy these equations/conditions exactly up to the order of truncation. This will allow us to retain only terms of $O(\delta)$ and lower. The coefficients will only contain explicit contributions from the leading order of the corrugated base flow. As such, this step can be achieved without knowing any details about the higher-order solutions of the base states.

In order for the corrugation terms to be of lower order than the first ε-order correction to the leading order (see the tangential stress condition below), we assume $\sigma \gg \varepsilon$, which for these scales, also decouples the core. From this point, we drop the primes for the disturbed quantities. The leading order of the film's governing equations become

$$0 = -p_z + \frac{m}{\lambda} w_{yy}, \quad 0 = p_y, \quad -u_y + w_z = 0. \tag{3.7a–c}$$

For the core, we have,

$$0 = -P_z + \frac{1}{\lambda}\nabla^2 W, \quad 0 = -P_r + \frac{1}{\lambda}\left(\nabla^2 U - \frac{U}{r^2}\right), \quad \frac{1}{r}(rU)_r + W_z = 0, \tag{3.7d–f}$$

subject to the boundary conditions.

On the wall,

$$y = -\sigma\phi, \quad w = 0, \quad u = 0. \tag{3.8a}$$

At the interface $r = S(z,t)$, we expand around the base state interface $S_b(z)$. After eliminating the base flow contributions, the leading terms in ε and δ for each boundary condition (other than the kinematic condition (3.6)) are:

Continuity of velocity to $O(\delta)$

$$-\xi\left(\frac{2}{m} + \sigma\bar{w}_y^{(1)}\right)_{y=1} + w(y = 1 - \sigma\eta) = -2\xi + W(r = 1) + O(\sigma\varepsilon), \quad U(r = 1) = O(\varepsilon). \tag{3.8b}$$

The tangential and normal stress balances to leading order $O(\delta/\varepsilon)$ are dominated by film variables:

$$-w_y(y = 1 - \sigma\eta) + \sigma\xi\bar{w}_{yy}^{(1)}(y = 1) = O(\varepsilon), \tag{3.8c}$$

$$\text{at } y = 1 - \sigma\eta, \quad p = \frac{J_0}{\lambda^2}(\xi_{zz} + \xi). \tag{3.8d}$$

In (3.8c), $\bar{w}^{(1)}$ is the coefficient of the $O(\sigma\varepsilon)$ axial valocity in (3.3a) for the film's base flow. Note that the normal stress does not contain the base flow's interface to leading order. From (3.2d), we can separate the interfacial curvature κ into the contribution of the base flow interface S_b

$$\kappa_b = \left[S_{bzz} - \frac{1}{S_b}(1 + S_{bz}^2)\right](1 + S_{bz}^2)^{-3/2}$$

plus the disturbed curvature

$$\kappa' = \delta\left\{\xi_{zz} + \frac{\xi}{S_b^2}(1 + S_{bz}^2) - \frac{2}{S_b}S_{bz}\xi_z - \xi_z S_{bz}\left[S_{bzz} - \frac{1}{S_b}(1 + S_{bz}^2)\right](1 + S_{bz}^2)^{-1}\right\}$$
$$\times(1 + S_{bz}^2)^{-3/2} + O(\delta^2).$$

The interaction terms, such as $\delta S_{bz}\xi_z \sim \delta\sigma\varepsilon$, in κ' that derive from S_z^2 are of higher order than $\delta(\xi_{zz} + \xi)$.

Solving for w and u from (3.7a–c) gives

$$w = \frac{\lambda}{2m} p_z y^2 + Cy + D, \tag{3.9a}$$

$$u = \frac{\lambda}{6m} p_{zz} y^3 + \tfrac{1}{2} C_z y^2 + D_z y + E, \tag{3.9b}$$

where $C = -(\lambda/m)p_z(1-\sigma\eta) + O(\sigma^2), D = -(\lambda/m)p_z\sigma\phi + O(\sigma^2)$ and $E = O(\sigma^2)$. Substitute (3.9) into (3.6) and use (3.8d) to derive the weakly nonlinear interface evolution inclusive of corrugation:

$$\xi_\tau + \frac{2}{m}\xi_z + \frac{J_0}{3m\lambda}(\xi_{zz}+\xi)_{zz} + \sigma\left[(\eta-\phi)\left(\frac{4}{m}\xi - \frac{J_0}{m\lambda}(\xi_{zz}+\xi)_z\right)\right]_z + \left(\frac{\delta}{\varepsilon}\right)\left(-\frac{2}{m}\xi\xi_z - \frac{J_0}{m\lambda}(\xi(\xi_{zzz}+\xi_z))_z\right) + O(\varepsilon, \sigma^2, \delta\sigma\varepsilon^{-1}) = 0. \tag{3.10}$$

At the leading order in δ, this equation recovers the linear analysis, which consists of the straight tube contribution and the $O(\sigma)$ term in square brackets due to the corrugation. The dependence on the corrugation is reflected by the variation of the base flow film thickness $(\eta-\phi)$ with z. The next order in δ (here $O(\delta/\varepsilon)$) gives the leading nonlinear terms. The first nonlinear term comes from the shear flow and is the usual (e.g. Papageorgiou *et al.* 1990) KS term. The second nonlinear term arises from the capillarity. Note that we remain in the laboratory frame (that is, we retain the convective term $(2/m)\xi_z$) instead of switching to a moving frame because of the presence of the corrugation. As we shall see in the next section, special forms of (3.10) apply to different scalings of J_0/λ, and thus of δ.

3.3. *Numerical methods*

To examine the impact of corrugation on the stability of the system, it is necessary to compare the numerical simulations for $\sigma = 0$ with those for $\sigma \neq 0$. Since the numerical solution must be calculated on a periodic domain, it is useful to employ spectral methods. Consider a periodic domain with period $2\pi/\beta$. We construct the solution to ξ as

$$\xi(z,\tau) = a_0(\tau) + \sum_{n=1}^{N}(a_n(\tau)\cos(\beta n z) + b_n(\tau)\sin(\beta n z)), \tag{3.11}$$

subject to a cosine wave initial condition $\xi(z,\tau=0) = A\cos(\alpha z)$ of the initial wavenumber α. At this juncture, in particular for comparing $\sigma = 0$ with $\sigma \neq 0$, we do not consider other forms of initial conditions, even though they may, in principle, lead to different behaviour. We choose the amplitude A of the initial interfacial profile relatively small (e.g. $A = 0.1$) so that its development appears to start within the linear regime. For $\sigma = 0$, the linear dispersion equation for mode n has a growth rate $(J_0/3m\lambda)(\beta n)^2(1-(\beta n)^2)$, which suggests that the modes with $\beta n > 1$ should decay with time and those with $\beta n < 1$ should grow as linearly unstable waves. For $\sigma \neq 0$, though, the wall wavelength $2\pi/k$ enters. The base flow term $\eta - \phi = h_1\cos(kz) + h_2\sin(kz)$, where h_1 and h_2 are known functions of k and J_0/λ (from WR). Although k can be an arbitrary real positive number independent of the choice of the initial wavenumber α, we choose it to have a rational ratio with α so as to guarantee that there is a period over which both the initial disturbance and the wall are periodic. We can choose β to be the greatest common divisor of k and α, and let $(k,\alpha) = (n_k, n_\alpha)\beta$ where n_k and

n_α are fixed integers. We also choose α belonging to the linearly unstable branch. With this choice, inserting (3.11) into (3.10) results in a system of ordinary differential equations for the amplitudes $a_n(\tau)$ and $b_n(\tau)$. We employ a fourth-order Runge–Kutta method to solve these temporal equations and use time steps from 2×10^{-4} to 10^{-3}, depending on the parameters. (For equation (4.5), which becomes stiff, we use Gear's method, with an initial step size of 10^{-15} and allow the method to vary the step size.) We choose the number N of modes retained to be large enough to resolve the spatial variation so that high harmonic modes decay. Typically, $N = 16$ is chosen for most simulations. We determine $a_n(\tau)$ and $b_n(\tau)$ to within 1% absolute error tolerance. We check spatial convergence by doubling N to verify that the spatial evolution does not change significantly.

4. Results and discussion

We now examine the numerical solutions for the weakly nonlinear interfacial evolution as given by (3.10). We turn to the applications mentioned above to motivate the parameter regimes for the numerics. In secondary oil recovery, *Re* is much smaller than one and typically $O(10^{-3})$, whereas J is order one or larger and typically $O(10^3)$ (Hammond 1983). According to Bretherton's analysis, the film thickness surrounding a slug of one fluid advancing into another fluid in a tube scales as $Ca^{2/3}$, which predicts $\varepsilon \sim 10^{-2} - 10^{-4}$ depending on the prefactor. Thus $J_0/\lambda = O(1)$, as well as slightly larger or smaller, are regimes of interest. In lung respiratory distress, recall than a thin liquid layer coats the cylindrical bronchioles. In distress, the naturally occurring surfactant DPPC is absent or inactive. It is thus unable to slow the time scale of the instabilities of the system that lead, in the terminal bronchioles, to either the film forming a lens and/or the elastic bronchiole collapsing, both of which block air flow (Otis *et al.* 1993). J for this problem is $O(10^3)$, $Re \sim 0.2 - 2$ for *Re* based on film properties and $\varepsilon \sim 0.02$ (Johnson *et al.* 1991). Thus, the lung problem has $J_0/\lambda \sim 1 - 1/\varepsilon$. Of interest is whether growth saturates in the weakly nonlinear regime (and if so, its shape) or continues beyond, suggesting possible film rupture.

4.1. *Strong interfacial tension case* $J_0/\lambda \sim O(1)$

Let us first consider the strong interfacial tension case $J_0/\lambda \sim O(1)$. In the absence of corrugation at $\sigma = 0$, (3.10) becomes

$$\xi_\tau + \frac{2}{m}\xi_z + \frac{J_0}{3m\lambda}(\xi_{zz} + \xi)_{zz} - \left(\frac{\delta}{\varepsilon}\right)\left(\frac{2}{m}\xi\xi_z + \frac{J_0}{m\lambda}(\xi(\xi_{zzz} + \xi_z))_z\right) = 0. \tag{4.1}$$

This equation is equivalent to those given by Aul (1989), Kerchman & Frenkel (1994), Kalliadasis & Chang (1994) and Kerchman (1995) in the small-amplitude disturbance limit. Note that there are weakly nonlinear terms deriving from both shear and capillarity. Unlike the KS equation, which only has a nonlinearity due to shear that can saturate linearly unstable waves, the presence of the capillary nonlinearity might, depending on the relative strength of the shear and capillarity, even amplify the linear instability. It might thus, in principle, cause growth beyond the weakly nonlinear regime. That is, even though the solutions to this equation may predict a long-term evolution whose interfacial disturbances may remain bounded, they may become comparable to the mean film thickness, and so equation (4.1) may not be uniformly valid in time (see Kalliadasis & Chang 1994; Kerchman 1995). In the analysis of Kerchman (1995), for relatively small order-one values of J_0/λ, the solutions show quasi-periodic or chaotic features similar to KS and thus the instability saturates

in the weakly nonlinear regime. For intermediate ranges of J_0/λ (about 0.7 in our notation), more film fluid can drain into the core. The film generally becomes more flattened but has larger bulges into the core. However, for even larger J_0/λ (about 0.9), strong core-bulging processes cause large interfacial amplitudes. Even though this solution remains numerically bounded, it is no longer weakly nonlinear and suggests that the core may snap off and break the CAF topology. These results qualitatively agree with Aul & Olbricht's (1990) experiments.

Even though Kerchman's work is based on a strongly nonlinear analysis, the weakly nonlinear equation (4.1) should show most of its qualitative features. When $\sigma \neq 0$, whether the corrugation or the nonlinearity dominates or whether both are comparable, depends on J_0/λ and the size δ of the interfacial perturbation. To bring the corrugation into the leading orders in the weakly nonlinear regime, we chose $\delta \sim \sigma\varepsilon$ so that the nonlinearity and the corrugation compete at the same order of σ in (3.10). For numerical computation, we thus choose $\sigma = 0.2$ and $\delta/\varepsilon = 0.15$ throughout this subsection. Note that even though δ is scaled by the corrugation, we numerically retain its size $\delta = 0.15\varepsilon$ when we compare solutions with and without ($\sigma = 0$) corrugation. That is, we first numerically confirm the features of (4.1) for $\sigma = 0$, $\delta = 0.15\varepsilon$ and then directly compare them with the case of (3.10) with corrugation. To do so, we remain in the laboratory frame throughout these simulations, even for $\sigma = 0$, rather than going to a moving frame, because it is more convenient for the corrugation case.

For $\sigma = 0$, as suggested by Kerchman (1995), we choose $J_0/\lambda = 0.7$ and $m = 1$ to ensure that the resulting long-time interfacial evolution is bounded in the weakly nonlinear regime. We impose an initial disturbance with small amplitude and a single unstable wavenumber of $\alpha = 0.6$. Figure 2(a) shows a series of snapshots of the spatial–temporal interfacial evolution. At the early stages of the evolution, the interface grows according to the linear theory. When the interfacial amplitude becomes sufficiently large (at about $\tau \sim 40$), nonlinear effects become important and the interface then undergoes a local curvature change owing to nonlinear coupling. As in Kerchman (1995), Papageorgiou *et al.* (1990), the upper part of the interface flattens and forms two humps and the lower part appears sharper with a high curvature around the trough. However, unlike the symmetric humps formed in the no-flow case by Hammond (1983), these two humps are asymmetric because of the base state shear flow at the leading order in ε. The long-term development is shown in figure 2(b). Steady waves are established at about $\tau \approx 100$, and travel with a speed $c \approx 2$ (owing to the retention of the linear convective term $(2/m)\xi_z$) in space. Note that even though the waves appear to be travelling backwards in the z-direction owing to the time between traces, they actually travel forwards, i.e. to the right. During the given time interval $\Delta\tau = 20$, the waves travel over a distance $c\Delta\tau \approx 40$. The resulting waves move a distance slightly less than four times the dominant wavelength $2\pi/\alpha (4 \times 2\pi/0.6 \approx 41.9)$. Therefore, the waves look as if they are travelling backwards.

Corrugation has the potential to complicate these pictures for $\sigma \neq 0$. Recall in the linear theory that the corrugation can respond to a short-wave disturbance by exciting the growth of long-wave wall harmonics of the initial disturbance at times of $O(\ln(1/\sigma))$. It may be interesting to see whether the nonlinearity accelerates or decelerates this corrugation-modified long-wave instability. As such, we select the following cases for a preliminary examination of the impact of corrugation on the solution of equation (3.10): $(\alpha, k) = (0.6, 1.8)$, $(1.2, 1.8)$, and $(1.8, 2.4)$. According to the linear theory, in the first case, the primary interfacial action is growth ($0.6 < 1$)

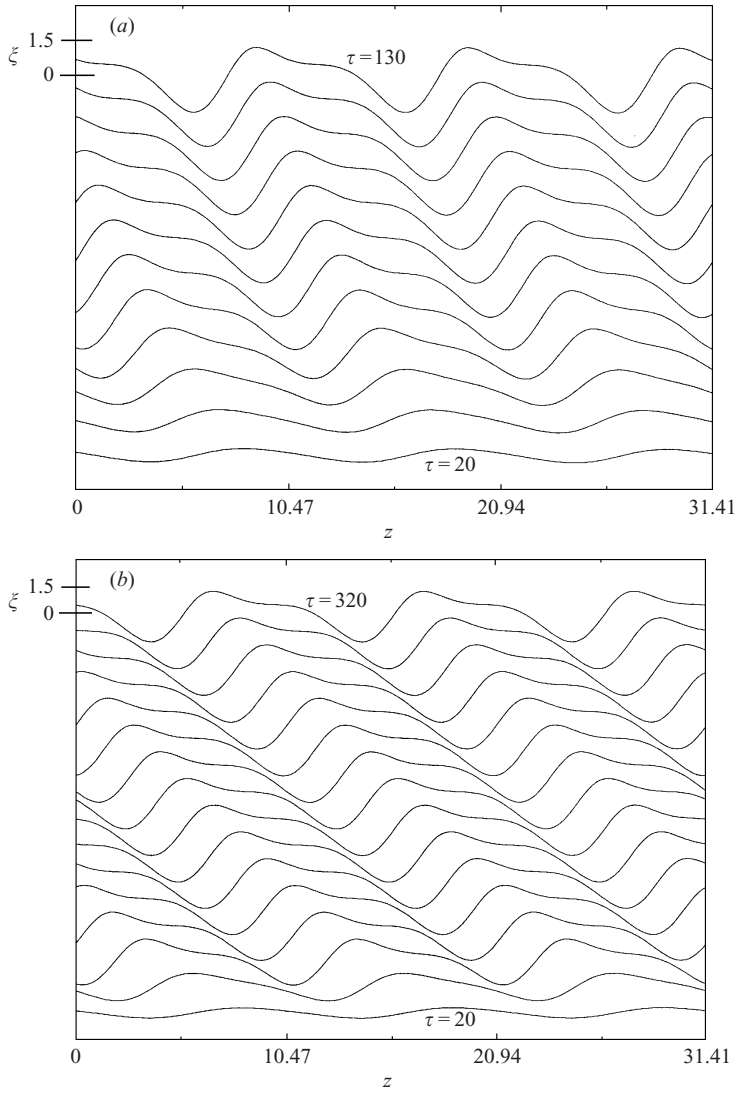

FIGURE 2. The weakly nonlinear interfacial evolution for the corrugation-free case for (*a*) short and (*b*) long times. Initial disturbance $\alpha = 0.6$ is linearly unstable. Nonlinear waves travel to the right with slightly less than one period per time interval between traces, thereby appearing to travel to the left. $J_0/\lambda = 0.7$, $\sigma = 0$, $\delta = 0.15\varepsilon$, interval between traces $\Delta\tau = 10$.

with the initial unstable wavelength later augmented by the higher harmonics of the wall corrugation. The latter two cases, however, will begin with a decaying initial disturbance that only at later times excites unstable harmonics whose resulting linearly unstable wavelengths coincide with those of the previous case. That is, all three of these cases have a dominant unstable wavenumber 0.6 in the linear regimes. Figures 3–5 show the spatial–temporal evolutions of these three cases. Before examining these figures in detail, we note that they all suggest that initial disturbances saturate.

At first glance, these long-term evolutions generally show the same dominant wavelength as and give similar interfacial shapes and travelling waves to the $\sigma = 0$ case. However, there are some different details in the local interfacial behaviour. In

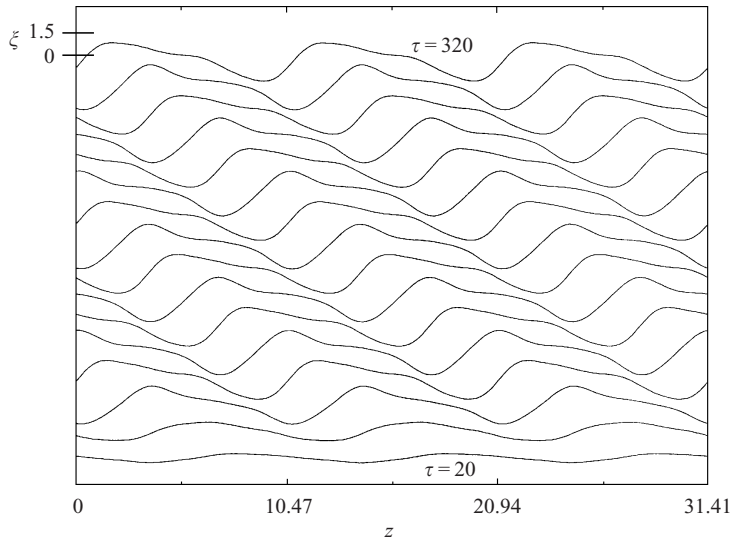

FIGURE 3. The weakly nonlinear interfacial evolution of the corrugation-free case for a linearly unstable initial disturbance $\alpha = 0.6$ and wall wavenumber $k = 1.8$. $J_0/\lambda = 0.7$, $\sigma = 0.2$, $\delta = 0.15\varepsilon$, interval between traces $\Delta\tau = 20$.

contrast to $\sigma = 0$, temporally oscillatory motions are present in the quasi-steady travelling waves as they pass the crests and troughs of the wall. In figure 3 with $(\alpha, k) = (0.6, 1.8)$, as in figure 2(b), the interface first amplifies the initial long-wave mode. However, it then develops quasi-steady travelling waves with temporal oscillations visible every two frames at 20 time unit intervals.

Upon imposition of a short wavelength disturbance such that $|\alpha - k| < 1$, cf. figures 4 and 5, the interface undergoes a transition from the decaying mode with an initial short-wavelength disturbance to a growing mode with a long wavelength in the linearly unstable regime. Thus, the time required to enter the nonlinear regime is, as expected, longer than in figure 3. For $(\alpha, k) = (1.2, 1.8)$ as shown in figure 4, the evolution reaches a quasi-steady state at $\tau \approx 200$, but then shows almost identical local oscillatory behaviour to figure 3. In the case of $(\alpha, k) = (1.8, 2.4)$, the transient state (not shown) takes even longer to develop because of the more rapid decay of the initial mode. The long-term interfacial motions are similar to those in figure 4 (note the similarity in shape between waves at $\tau = 300$ in figures 3 and 4, and $\tau = 400$ in figure 5), but the quasi-steady state behaviour in figure 5 is rather different from those in the previous cases. There are four frames per cycle of oscillatory motions and they have stronger modulations than do the earlier cases. The different numbers of traces per cycle and split peaks in every fourth trace appear to coincide with the more frequent occurrence of the wall crests and troughs for the large wall wavenumber k.

Figure 6 shows the case of $(\alpha, k) = (0.3, 2.4)$ whose unstable initial wave is 0.3, but whose wall wavenumber is the same as in figure 5. Here, the waves appear more intricate. As shown in figure 6(b), they appear to require eight frames of an oscillatory cycle when $\tau = 500 \sim 660$. This intricacy is not surprising since the linearly unstable wave present is double the size of the previous cases and thus sees more of the wall's corrugation per disturbance period. Note that all of these corrugation cases have a similar travelling wave speed, $c \approx 2$, with a small corrugation correction for each case. The longer the dominant wavelength, the longer the time a wave travels

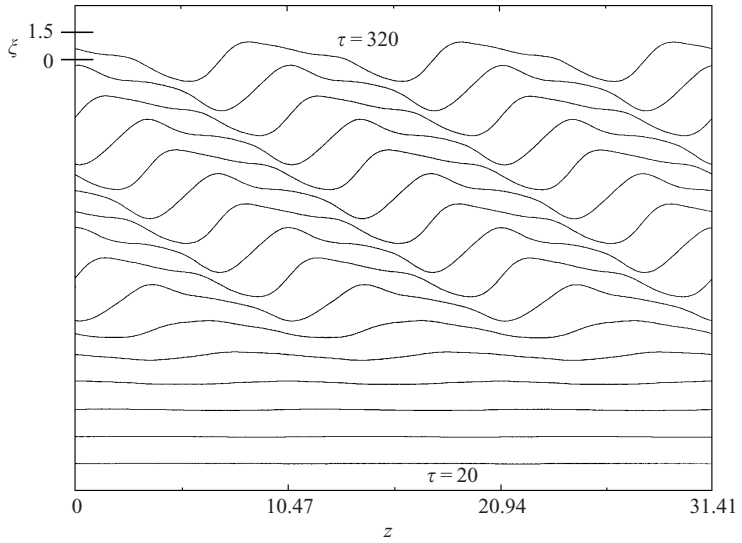

FIGURE 4. The weakly nonlinear interfacial evolution with corrugation-free case for a linearly stable initial disturbance $\alpha = 1.2$ and wall wavenumber $k = 1.8$. Linear coupling to the walls' corrugated wavelength excites unstable waves $|\alpha - k|$ for times of order $\ln(1/\sigma)$. $J_0/\lambda = 0.7$, $\sigma = 0.2$, $\delta = 0.15\varepsilon$, $\Delta\tau = 20$.

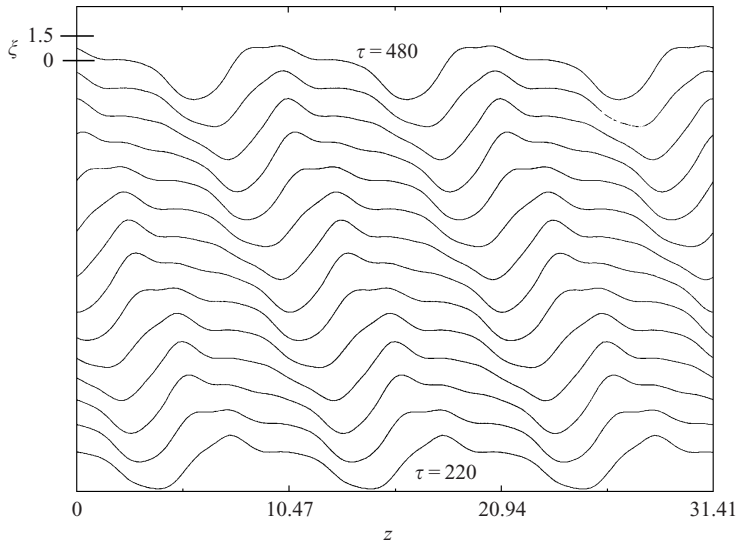

FIGURE 5. Long time weakly nonlinear interfacial evolution with corrugation-free case for a linearly stable initial disturbance $\alpha = 1.8$ and wall wavenumber $k = 2.4$. Linear coupling to the walls' corrugated wavelength excites unstable waves $|\alpha - k|$ for times of order $\ln(1/\sigma)$. $J_0/\lambda = 0.7$, $\sigma = 0.2$, $\delta = 0.15\varepsilon$, interval between traces $\Delta\tau = 20$.

over a distance equal to its wavelength. On the other hand, the shorter the wall wavelength, the more frequently the interface with a longer wavelength encounters the wall's crests and troughs; therefore the time periodicity becomes longer. This time periodicity is roughly proportional to the ratio k/α_d of the wall wavenumber to the dominant wavenumber α_d. For the same wall waviness $k = 2.4$ as in figures 5 and 6, the dominant wavelength in figure 6 is twice that in figure 5. The resulting oscillation

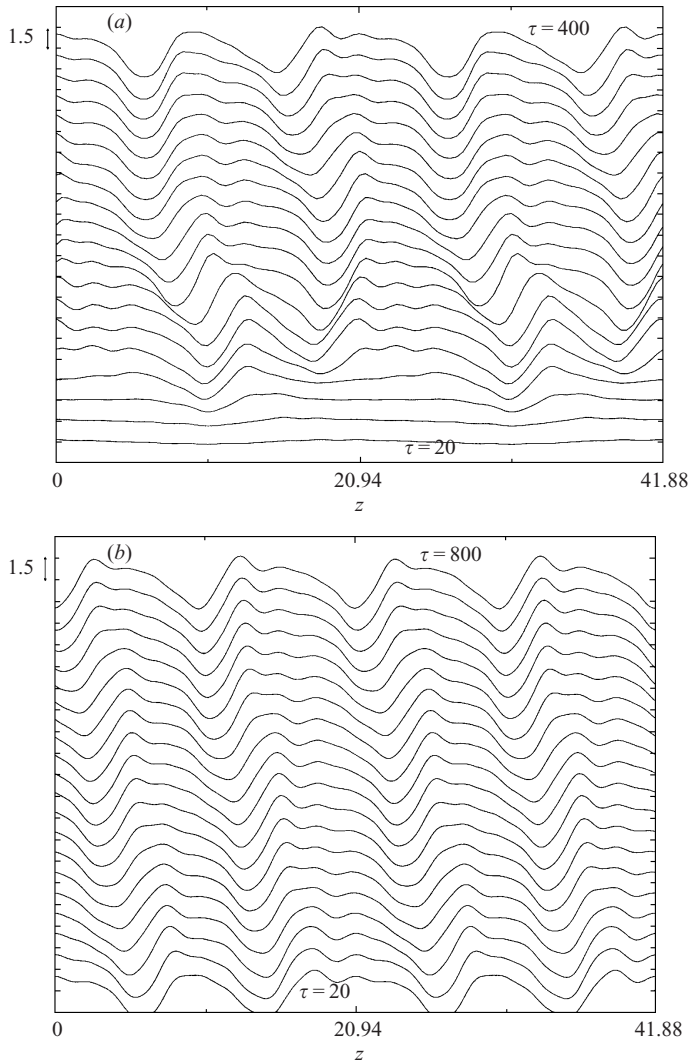

FIGURE 6. Same as figure 5, but for a linearly unstable initial perturbation $\alpha = 1.8$ at (*a*) short and (*b*) longer times.

period in figure 6 is double that in figure 5. Similarly, for the same dominant wave as in figures 4 ($k = 1.8$) and 5 but for a different k, we estimate the time period in figure 5 as 1.5 (or 2) times that in figure 4.

In summary, for $J_0/\lambda = 0.7$, these results show that the nonlinear saturation overcomes the continual excitation of new unstable long waves by the corrugation and leads to steady or quasi-steady travelling waves. That is, the film/core arrangement should persist.

If we increase the scaled inverse capillary number as $J_0/\lambda \gg 1$, the capillary force overwhelms the effect of the base flow, and we might expect the system to approach Hammond's limit. In this limit, the interface in the leading-order base state is cylindrical, i.e. $\eta = 0 + O(J_0/\lambda)^{-1}$. Assuming $J_0/\lambda \gg \sigma^{-1}$ and restricting the time scale to $O(J_0/\lambda)^{-1}$, we find that the base flow drops out of the leading-order weakly

nonlinear equation:

$$\xi_\tau + \frac{J_0}{m\lambda}\{\tfrac{1}{3}(\xi_{zz}+\xi)_{zz} + \sigma[\phi(\xi_{zzz}+\xi_z)]_z - \frac{\delta}{\varepsilon}[\xi(\xi_{zzz}+\xi_z)]_z\} + O(1) = 0. \qquad (4.2a)$$

The presence of the corrugation in the linear theory can cause a resonance that amplifies the instability to $O(\sigma)$ from $O(\sigma^2)$ for some ranges of wavelengths of the disturbance and the wall (WR, § 3). For convenience, let $\tau \to (m\lambda/J_0)\tau$. The leading order of (3.2a) becomes

$$\xi_\tau + \tfrac{1}{3}(\xi_{zz}+\xi)_{zz} + \sigma[\phi(\xi_{zzz}+\xi_z)]_z - \left(\frac{\delta}{\varepsilon}\right)[\xi(\xi_{zzz}+\xi_z)]_z = 0. \qquad (4.2b)$$

At $\sigma = 0$, this equation reduces to the weakly nonlinear version of Hammond's equation, that is, with a linearized version of the cubic nonlinearity. Consider an interface with a single long wavelength that is linearly unstable. For $\sigma = 0$, the capillary term can be rearranged as

$$\left(1 - 3\frac{\delta}{\varepsilon}\xi\right)(\xi_{zz} + \xi_{zzzz}) - 3\left(\frac{\delta}{\varepsilon}\right)\xi_z(\xi_z + \xi_{zzz}).$$

The first of these terms involves

$$h^3 = \left(1 - \frac{\delta}{\varepsilon}\xi\right)^3 \approx \left(1 - 3\frac{\delta}{\varepsilon}\xi\right) + O\left(\left(\frac{\delta}{\varepsilon}\right)^2\right),$$

the cube of the film thickness h. This term slightly amplifies the growth of the interface's trough (with $\xi < 0$) and slightly suppresses the growth at its crest (with $\xi > 0$) in the weakly nonlinear regime relative to the linearly growing interface. This leads to a flatter crest and steeper trough. The second term would come into play should a small-amplitude, short-wave depression occur by fluctuation in the crest. Except at the points in the depression where $\xi_z = 0$, the first and third derivatives are of opposite signs, with the third derivative of larger magnitude. This would cause the disturbance to grow until the first derivative was comparable to the third derivative or until the local curvature corresponded to a wavelength of at least one. As a result of both of these terms, the interface shape forms two shallow symmetric humps near the wall and a deep trough protruding into the core.

The numerical solution of (4.2b) (with $\alpha = 0.7$ and $\sigma = 0$) is shown in figure 7. The rate of change of the solution slows down markedly at $\tau \approx 90$. The interface shape is similar to the solution with Hammond's retention of the full cubic factor, although the evolutions in Hammond's case do not reach a steady state, their growth in the nonlinear regime is very slow. For the case with corrugation ($\sigma \neq 0$), we choose $k = 1.4$ so that the resonance in the linear theory occurs at the initial wavenumber $\alpha = 0.7$ of the disturbance: Even ($0.1\cos(\alpha z)$) and odd ($0.1\sin(\alpha z)$) (there is no difference for $\sigma = 0$) parities (relative to the wall) of the initial condition are also chosen for comparison purposes, and the corresponding results are presented in figures 8(a) and 8(b), respectively. Note that the wall profiles drawn in figure 8 are not in true scale and only indicate a relative phase between the interface and the wall. In general, the evolution for $\sigma \neq 0$ is more amplified than that for $\sigma = 0$. For an even initial interfacial profile, the interface appears to reach a steady state at $\tau \approx 220$. The humps all appear more pronounced than those for $\sigma = 0$. On the other hand, the odd initial disturbance leads to a more unstable evolution than the even case. ξ is order 10 at $\tau = 100$, which means the interfacial amplitude $\delta\xi \sim 1.5\varepsilon$, clearly beyond the weakly

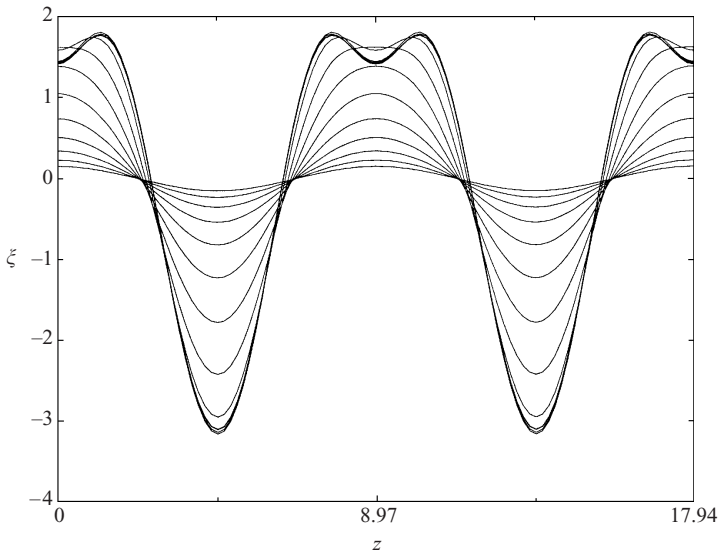

FIGURE 7. Weakly nonlinear interfacial evolution for the corrugation-free case in the limit where surface tension forces predominate over shear forces, i.e. no flow. Initial disturbance $\alpha = 0.7$ is linearly unstable. $\Delta\tau = 5$. Interfacial growth appears to saturate by time 100.

nonlinear regime. When the two humps form at the crest for the odd initial condition, their growth seems to accelerate with time rather than slowing down. Thus, this case shows no sign of approaching a steady state. In a qualitative comparison with Gauglitz & Radke (1990), the upper part of our odd initial interfacial profiles corresponds to their 'thick–thin' case, which also showed a similar qualitative feature and a faster growing evolution. Figure 8(*c*) chooses an initial condition $(0.1/\sqrt{2})(\cos(\alpha z)+\sin(\alpha z))$ with both even and odd profiles together. The evolution also shows features similar to the odd case in figure 8(*b*) and grows faster than the even case in figure 8(*a*). It seems that the odd initial condition, where the interfacial peaks and valleys are mostly in phase with those of the wall, triggers more instability. Note that we restrict our attention to the above no-flow limit (4.2*a*) for time scales $O(\lambda/J_0)$ because the system has already left the weakly nonlinear regime. For even longer time scales, the weak base flow will certainly alter the in or out of phase character discussed. It may continue to drive the film-drainage process even longer and form even larger lobes into the core, as seen by Kalliadasis & Chang (1994) or Kerchman (1995).

4.2. *Less strong interfacial tension case* $\varepsilon \ll J_0/\lambda \ll 1$

As shown by Sivashinsky & Michelson (1980) for the flow of a thin film on a vertical wall and Frenkel *et al.* (1987) for a core–annular flow of fluids of matched densities and viscosities without wall corrugation, an intermediately strong interfacial tension $\varepsilon \ll J_0/\lambda \ll 1$ can lead to the KS equation. The weakly nonlinear interfacial evolution at $\sigma = 0$ is governed by

$$\xi_\tau + \frac{2}{m}\xi_z + \frac{J_0}{3m\lambda}(\xi_{zz}+\xi)_{zz} - \left(\frac{\delta}{\varepsilon}\right)\frac{2}{m}\xi\xi_z = 0, \tag{4.3}$$

which, upon switching to a travelling reference frame, is just KS, an equation whose dynamics have been well studied (e.g. Hyman & Nicolaenko 1986; Smyrlis & Papageorgiou 1990; Papageorgiou & Smyrlis 1991). Without the capillary-derived nonlin-

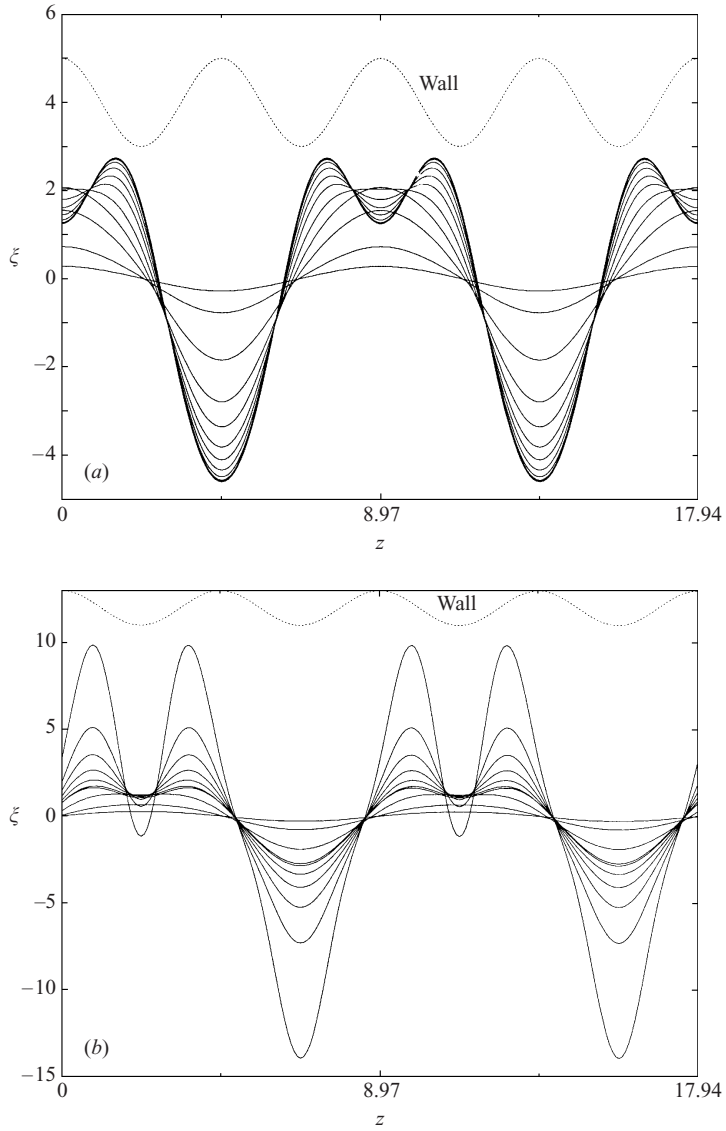

FIGURE 8 (*a*, *b*). For caption see facing page.

earity that causes film drainage into large troughs, the shear nonlinearity $\xi\xi_z$ steepens and thereby shortens the growing linearly unstable long waves and the longitudinal component of capillarity saturates their growth. Extensive numerical investigations on a periodic domain (Sivashinsky & Michelson 1980; Frisch, She & Thual 1986; Hyman & Nicolaenko 1986; Smyrlis & Papageorgiou 1990; Papageorgiou & Smyrlis 1991) have shown that depending on the number of linear unstable waves per period, the solution generally exhibits complex chaos (long periods), dynamics such as uni- or multi-modal travelling waves, oscillations, or some combinations of these (Hyman & Nicolaenko 1986). However, as demonstrated by Kawahara (1983), the addition of a linear dispersion term (e.g. a third derivative term) to KS can regularize the chaotic motions and form travelling waves. Similar conclusions for more complicated dispersion forms arise from Papageorgiou *et al.* (1990) and Kerchman (1995).

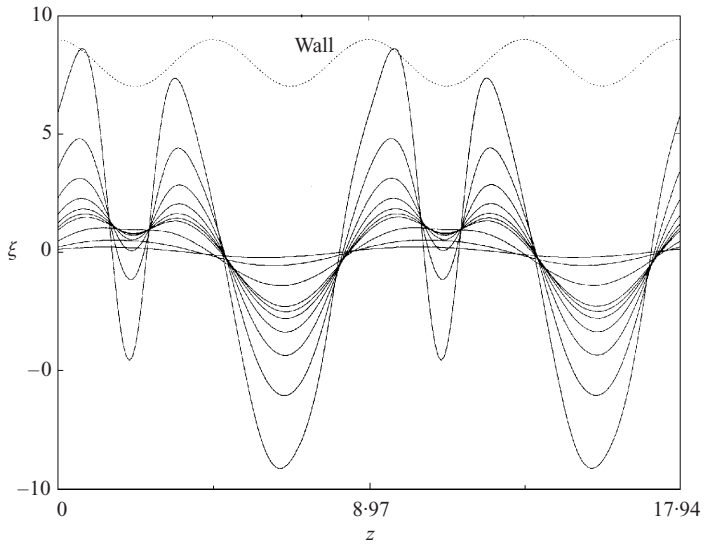

FIGURE 8. Interfacial evolution in the strong surface tension limit for the case with corrugation. Initial condition (*a*) in phase (*b*), out of phase, or (*c*) mixed with wall at double its wavelength. Wall shown not to scale. Corrugation amplifies interfacial evolution relative to the corrugation-free case. In phase initial condition appears to lead to a steady interface; out of phase conditions seem to grow beyond the weakly nonlinear regime. $\sigma = 0.2,\ \alpha = 0.2,\ \delta = 0.15\varepsilon$, (*a*) $\Delta\tau = 20$, or (*b*, *c*) 10.

In the presence of wall corrugation, the base interface follows the shape of the wall ($\eta - \phi = -(J_0/6\lambda)(\phi_{zzz} + \phi_z) + O(J_0/\lambda)^2$) to leading order. Thus, the film thickness is uniform and the film flow is locally parallel to leading order in σ and J_0/λ. To derive a weakly nonlinear equation that has a leading-order corrugation contribution, now of order $\sigma J_0/\lambda$, we restrict our attention to a scaling $\sigma\varepsilon \gg \delta$. Under these conditions (see equation (3.10)), the capillary nonlinearity is of higher order ($O(\delta J_0/\lambda\varepsilon)$) than the convective corrugation contribution ($O(\sigma J_0/\lambda)$), as is the capillary part of the corrugation ($O(\sigma(J_0/\lambda)^2)$). Thus, we may choose δ to be either of order $\varepsilon J_0/\lambda$ or $\varepsilon\sigma J_0/\lambda$. In the former (latter) case, the nonlinear term competes with capillarity (corrugation). Let us examine the latter case more closely. For $\delta \sim \varepsilon\sigma J_0/\lambda$, capillarity is the only leading-order term, and both the nonlinear and corrugation terms contribute at the first correction. Such a nonlinear term competes with the capillary instability only when the time scale $\tau \sim O(\sigma J_0/\lambda)^{-1}$. However, by this time, ξ has grown to be $O(e^{1/\sigma})\xi(\tau = 0)$, and thus causes the overall interfacial amplitude $\delta\xi$ to be $O(\sigma\varepsilon e^{1/\sigma} J_0/\lambda)$. This is beyond the size of δ presumed in (3.10). Therefore, we choose $\delta \sim \varepsilon J_0/\lambda$ in the presence of corrugation and arrive at

$$\xi_\tau + \frac{2}{m}\xi_z + \frac{J_0}{3m\lambda}(\xi_{zz} + \xi)_{zz} - \left(\frac{\sigma J_0}{\lambda}\right)\frac{2}{3m}\left[(\phi_{zzz} + \phi_z)\,\xi\right]_z - \left(\frac{J_0}{\lambda}\right)\frac{2}{m}\xi\xi_z + O\left(\frac{\varepsilon J_0}{\lambda}\right) = 0. \tag{4.4}$$

The corrugation term is now of higher order than the nonlinear term. Thus, at leading order in J_0/λ, the evolution is primarily determined by the KS mechanism and, in the absence of other effects, we expect the linear instability to saturate. There are a number of questions that arise from (4.4). At these scales, corrugation ($\sigma \neq 0$) contributes a purely dispersive correction to the growth rate at $O(\sigma(J_0/\lambda)^2)$. In view of Kawahara & Toh's (1988) observation (also seen by Papageorgiou *et al.* 1990) that a dispersive term can regularize otherwise chaotic motions, this observation holds out

the possibility that corrugation may have a similar regularizing effect. On the other hand, the linear theory showed that $\sigma \neq 0$ can allow even short-wavelength interfacial pertubations α to excite growing long waves $\alpha \pm nk$ (k is the wavenumber of the wall), when $-1 < \alpha \pm nk < 1$ (n is an integer). Thus, the continual self-generation of perturbations of various wavelengths may cause solutions on periodic domains of a size that would lead to regular nonlinear travelling waves for a unimodal initial condition as used (e.g. by Hyman & Nicolaenko 1986; Smyrlis & Papageorgiou 1990; Papageorgiou & Smyrlis 1991) to become chaotic.

A numerical solution is again necessary to examine these possibilities. We begin by recasting (4.4) in the canonical form used by previous authors for KS so as to make explicit the length scale of periodicity of the numerical solution. Since all of the terms in (4.4) (except the $O(1)$ convective term) are $O(\sigma J_0/\lambda)$ or higher, we introduce a long time scale $\tau \sim O(J_0/\lambda)^{-1}$ to access their dynamics. Letting $x = z\sqrt{v}$, $\Theta = 6\xi/\sqrt{v}$, $T = (vJ_0/3m\lambda)\tau$ transforms (4.4) into

$$\Theta_T + \frac{6\lambda}{J_0 v^{1/2}}\Theta_x - \Theta\Theta_x + (\Theta_{xx} + v\Theta_{xxx}) - 2\sigma\left[\frac{1}{v}f_1\Theta + \frac{1}{\sqrt{v}}f_2\Theta_x\right] = 0, \qquad (4.5)$$

where both $f_1 = f_1(kx/\sqrt{v}) = \phi_{xxxx}+\phi_{xx}$ and $f_2 = f_2(kx/\sqrt{v}) = \phi_{xxx}+\phi_x$ represent the contributions of the corrugated wall. A brief interpretation is warranted. Balancing the circumferential Θ_{xx} and longitudinal curvatures $v\Theta_{xxxx}$ yields a length scale $v^{1/2}$ in the z- (now x-) domain. The critical wavenumber in these units and the number of unstable waves in the periodic domain (of length 2π) in x on which we solve (4.5) are both $1/\sqrt{v}$. The amplitude of Θ at which the nonlinearity becomes important can also be estimated as $v^{-1/2}$ by balancing the nonlinear and capillary terms. A balance with the unsteady term gives the time scale v. The wall's wavenumber k enters via ϕ and is taken as an integral number n_k of $\sqrt{v}$, i.e. $k = n_k\sqrt{v}$. Previous authors have mapped out the qualitative behaviours of solutions to KS as a function of this sole parameter v for cosine initial conditions of unit magnitude in these units. Since KS is nonlinear, these qualitative behaviours may be initial-condition dependent. These authors (e.g. Smyrlis & Papageorgiou 1990) find that to obtain chaotic motions, long periodic domains, i.e. v small, are required, although below the largest v for chaos, there are numerous intervals of v where solutions exhibit various types of regularity, interspersed within v regions characteristic of chaos. In our numerical simulations, we typically use 36 modes to solve (4.5) and apply Gear's method to solve the temporal evolutions within 0.1 % absolute error tolerance.

We begin by verifying that the linear portion of equation (4.5) also has the property that short-wavelength α disturbances can, via coupling to $\sigma \neq 0$ corrugation wall harmonics, excite unstable long-wave growth. Figure 9 shows the evolution for $v = 0.03$, $\sigma = 0.2$. $J_0/\lambda = 0.02$ and the nonlinear term zeroed out, of an initial short-wave cosine disturbance with $\alpha_{initial} = 6 > \alpha_{crit}(= 5.77)$ and amplitude 0.1 for a wall having $n_k = 4$. Figures 9–14 show instantaneous interfacial shapes, beginning with the initial condition as the lowest curve and with subsequent times sequentially displaced in the upward direction. As expected, the initial perturbation decays, and at times beyond $T \approx 3.5$ ($\ln(1/\sigma) \sim 1.6$), the wave $\alpha - n_k = 6 - 4 = 2$ begins to grow linearly. Next, we consider $v = 0.0222$, within a band of values that lead to 5-wave travelling waves (see figure 10(a) and Smyrlis & Papageorgiou 1990), between regions of v that yield chaotic solutions, for KS, i.e. for $\sigma = 0$. Upon activating the corrugation, i.e. changing σ from 0 to 0.2, with all other parameters unchanged, the dynamics loose their regularity, as figure 10(b) demonstrates. This suggests that

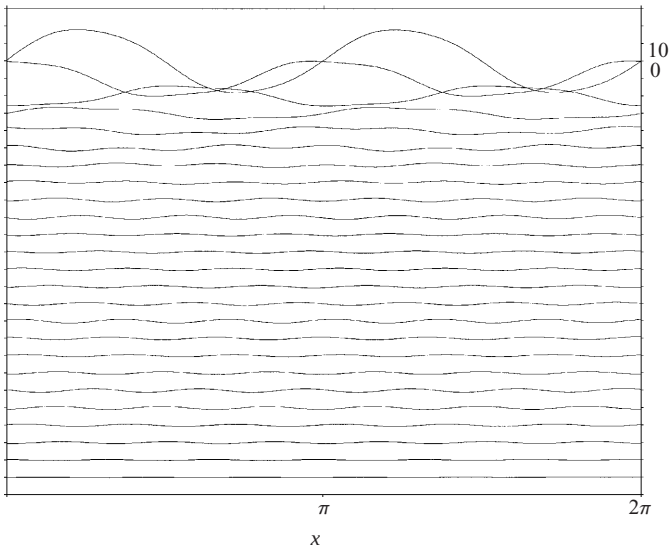

FIGURE 9. Solution of equation (4.5) for the linear interfacial evolution (without the term $\theta\theta_x$) for the case with corrugation where flow is dominant over surface tension forces. Initial short-wave disturbance $\alpha = 6$ is linearly stable. Coupling to wall's harmonics excites long waves at times of order $\ln(1/\sigma)$. $J_0/\lambda = 0.02,\ \sigma = 0.2, v = 0.03,\ n_k = 4$, initial amplitude $= 0.1,\ \Delta T = 0.16$.

the regularity exhibited by KS for this periodic domain in response to a single-mode initial condition of unit magnitude can be destroyed by the generation of multiple wavelength perturbations by the corrugation's coupling to the wall harmonics. Figure 11 confirms that for the parameters of figure 10(a), but for a bimodal initial condition, i.e. containing the disturbance of figure 10(a) with the excited wave from figure 10(b) superimposed upon it, even KS appears to exhibit chaos.

Finally, we examine a v value corresponding to chaotic solutions in response to a cosine initial condition of unit magnitude. Our goal is to see if we can find a case opposite to that of the last paragraph, i.e. where the dispersion introduced by the leading-order corrugation can regularize otherwise chaotic solutions. Although we were unable to find such a regularization of the long time behaviour over the time scale of our simulation, we were able to see an interesting effect on the approach to chaos. Figure 12 solves (4.5) at $\sigma = 0$ (no corrugation) with an odd-parity initial condition $\Theta(x, T = 0) = -0.1\sin(x)$ for $v = 0.027$ and $J_0/m\lambda = 0.02,\ T = 1$; these numbers correspond to $\tau \sim 5000$ and initial amplitude $\xi = 0.003$ in (4.4). This typical KS evolution exhibits temporal and spatial chaotic motions with four or five wavelengths in a period of 2π after growth beyond the linear regime, although some time snapshots appear almost periodic, e.g. $T = 4.8,\ 7.2$ and 8.8. Next, we impose a small corrugation $\sigma = 0.2$ for wall wavenumber $k = 0.1643n_k$ and initial condition $\Theta(x, T = 0) = -0.1\sin(x)$. For $n_k = 2$ (figure 13) there is a long period where the interface shape is relatively flat and static before abruptly changing to chaos. Such an almost static period also occurs for $n_k = 3$ (figure 14), but there it occurs between chaotic periods and for a shorter duration than for $n_k = 2$. However, for larger $n_k = 4$, 5 (not shown), the evolution is qualitatively almost identical to figure 12. Thus, the order $\sigma(J_0/\lambda)^2$ dispersion introduced by the corrugation for the scaling $\varepsilon \ll J_0/\lambda \ll 1$ appears to be too weak to regularize an otherwise chaotic solution at long times in our simulations, but they do appear to influence the dynamic approach to chaos.

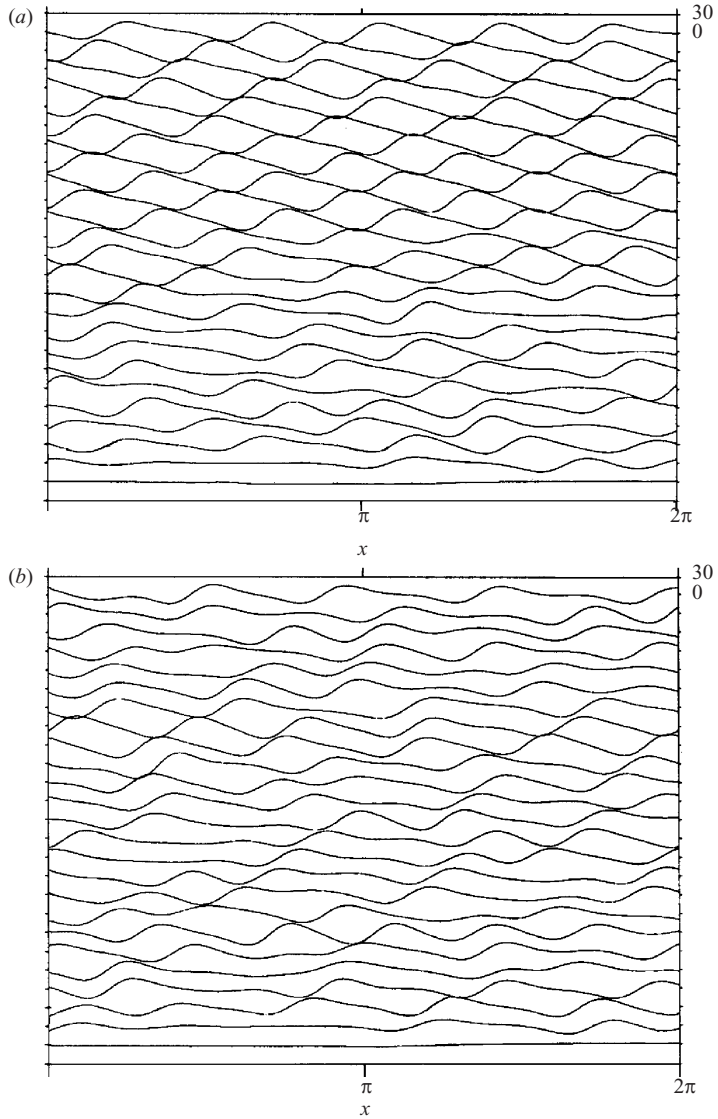

FIGURE 10. Corrugation can make chaotic an otherwise regular interfacial motion. Solution of (4.5) for $v = 0.0222$ such that the interface is (a) non-chaotic in the corrugation-free case ($\sigma = 0$) and (b) chaotic for $\sigma = 0.2$. $n_k = 5$, initial amplitude $= 1.0$, $\Delta T = 0.4$.

Whether there is a longer time periodicity corresponding to this weak dispersion is unclear without much longer simulations. We do note, however, that artificially multiplying the corrugation term by 100 does indeed yield an (unphysically large) dispersion that regularizes the interface (not shown), as would be anticipated from Kawahara & Toh (1988).

5. Summary and conclusions

We have investigated the weakly nonlinear interfacial stability of a core–annular flow in the presence of an asymptotically thin annulus and small corrugation. This

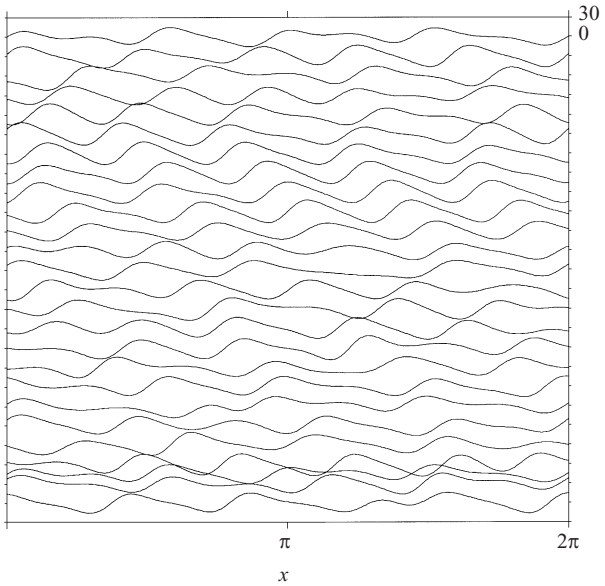

FIGURE 11. Solution to the KS equation (Equation (4.5) with $\sigma = 0$) for the same parameters as figure 10, but with a different initial condition indeed yields chaotic solutions. Initial conditions chosen to be the wave that is excited by corrugation in figure 10(*b*).

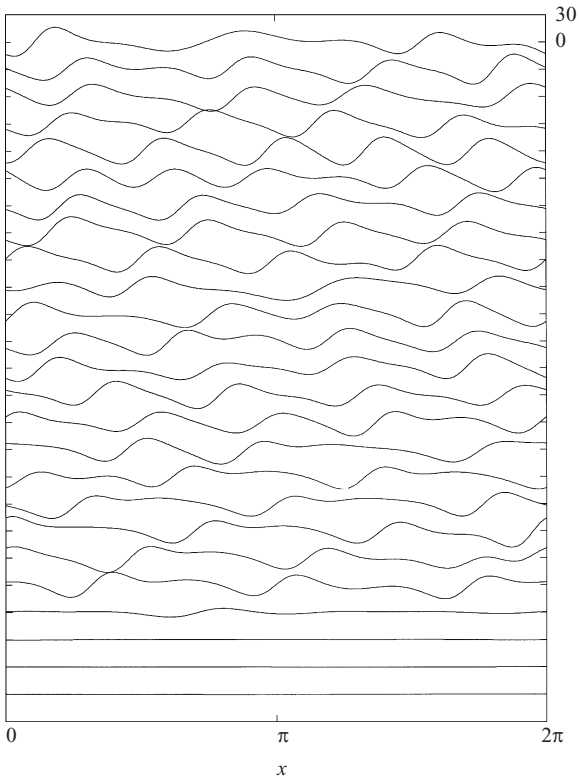

FIGURE 12. Chaotic interfacial evolution according to equation (4.5) without corrugation. $\sigma = 0,\ \nu = 0.027$, initial amplitude $= 0.1$, $\Delta T = 0.4$.

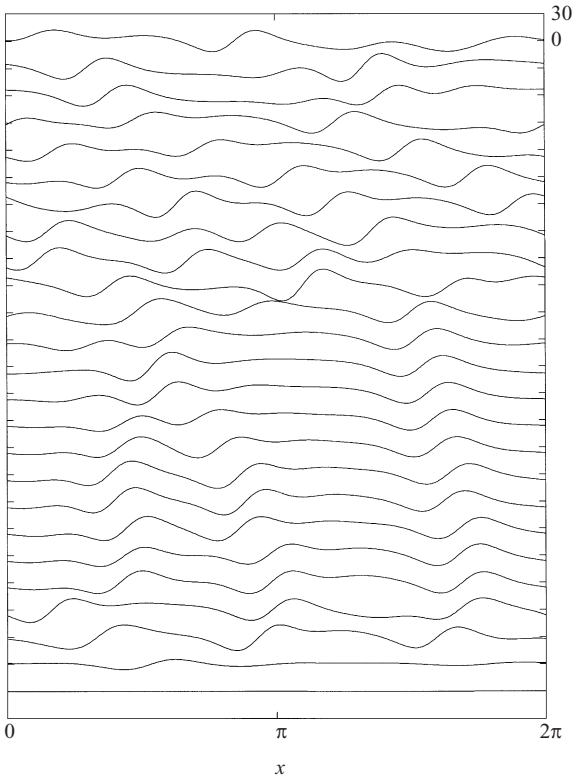

FIGURE 13. Same as figure 12, but with small corrugation $\sigma = 0.2$, $n_k = 2$ and $\Delta T = 0.8$. Onset of chaos is delayed, apparently by the weak dispersion term that is activated by corrugation.

flow is a model for liquid–liquid displacements in pores as occur in secondary oil recovery and for the film–lens transition of the liquid lining in the terminal lung bronchioles. Of interest is the stability of the core–annular arrangement, and thus of the linear and nonlinear interfacial stability and shape. Here, and in WR, we focus on the impact of the non-uniformity of the radii of the pore or bronchiole. The linear stability of this system (WR) showed that the corrugation facilitated the coupling of the initial disturbance α to wall harmonics of k which, for the right choices of α and k, could potentially excite unstable long waves. The questions motivating this study included whether this continuous generation of new unstable long waves by the corrugation could be saturated by the wave steepening nonlinear KS mechanism. For $O(1)$ values of the parameter J_0/λ, the ratio of surface tension to viscous forces, multiplied by the square of the scaled mean film thickness, the answer was yes, and the evolution acquired a temporal periodicity for $\sigma \neq 0$ that corresponded to the otherwise steady waves passing through the wall's crests and troughs. Moreover, a capillarity-derived weakly nonlinear term in addition to the usual kinematic-condition-derived weakly nonlinear term biases the dynamics away from chaos and towards regularized travelling waves.

For $J_0/\lambda \gg 1$, capillarity dominates flow, and the weakly nonlinear version of Hammond's equation results. Numerical solution suggests an instability that grows beyond the weakly nonlinear regime, possibly to snapoff. Corrugation changes this picture, in that, for initial conditions in phase with the wall, the growth seems to slow, but for most initial conditions not aligned with the wall, the growth seems to be even

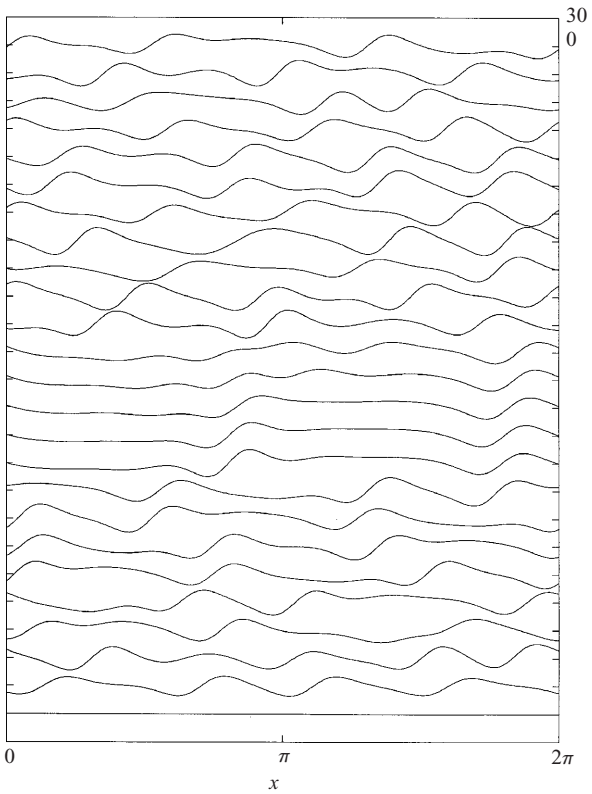

FIGURE 14. Same as figure 13, but with $n_k = 3$. A period of nearly flat interfacial profiles occurs between periods of apparently chaotic interfacial motion.

faster. Finally, for $\varepsilon \ll J_0/\lambda \ll 1$, although the corrugation growth rate correction to leading order is dispersive, it appears too weak to regularize otherwise chaotic motions of the governing weakly nonlinear KS equation. It does, however, appear to slow the development to chaos for walls where the waves are not too short. On the other hand, the corrugation's excitation of unstable long waves by the coupling of the initial perturbation to the wall's periodicity does appear capable at this order of overwhelming some situations/initial conditions that would have otherwise evolved to travelling waves and instead causes the system to become chaotic.

REFERENCES

AUL, R. W. 1989 The motion of drops and long bubbles through small capillaries: coalescence of drops and annular film stability. PhD thesis, Cornell University Ithaca, NY.

AUL, R. W. & OLBRICHT, W. L. 1990 Stability of a thin annular film in a pressure-driven, low Reynolds number flow through a capillary. *J. Fluid Mech.* **215**, 585–599.

BRETHERTON, R. P. 1961 The motion of long bubbles in tubes. *J. Fluid Mech.* **10**, 166–188.

CHANDRASEKHAR, S. 1968 *Hydrodynamic and Hydromagnetic Stability*. Oxford University Press.

CHANG, H.-C. 1987 Evolution of nonlinear waves on vertically falling films – a normal form analysis. *Chem. Engng Sci.* **42**, 515–533.

CHEN, K., BAI, R. & JOSEPH, D. D. 1999 Lubricated pipeline. Part 3. Stability of core–annular flow in vertical pipes. *J. Fluid Mech.* **214**, 251–286.

DASSORI, C. G., DEIBER, J. A. & CASSANO, A. E. 1984 Slow two-phase flow through a sinusoidal channel. *Intl J. Multiphase Flow* **10**, 181–193.

Frenkel, A. L., Babchin, A. J., Levich, B. G., Shlang, T. & Sivashinsky, G. I. 1987 Annular flows can keep unstable films from breakup: nonlinear saturation of capillary instability. *J. Colloid Interface Sci.* **115**, 225–233.

Frisch, U., She, S. & Thual, O. 1986 Viscoelastic behaviour of cellular solutions to the Kuramoto–Sivashinsky model. *J. Fluid Mech.* **168**, 221–240.

Gauglitz, P. A. & Radke, C. J. 1988 An extended evolution equation for liquid film break up in cylindrical capillaries. *Chem. Engng Sci.* **43**, 1457–1465.

Gauglitz, P. A. & Radke, C. J. 1990 The dynamics of liquid film break up in constricted cylindrical capillaries. *J. Colloid Interface Sci.* **134**, 14–40.

Georgiou, E. C., Maldarelli, C., Papageorgiou, D. T. & Rumschitzki, D. S. 1992 An asymptotic theory for the linear stability of a core–annular flow in the annular limit. *J. Fluid Mech.* **243**, 653–677.

Halpern, D. & Grotberg, J. B. 1993 Surfactant effects on fluid-elastic instabilities of liquid-lined flexible tubes: a model of airway closure. *J. Biomech. Engng* **115**, 271–277.

Hammond, P. S. 1983 Nonlinear adjustment of a thin annular film of viscous fluid surrounding a thread of another within a circular cylindrical pipe. *J. Fluid Mech.* **137**, 363–384.

Hooper, A. P. & Grimshaw, R. 1985 Nonlinear instability at the interface between two viscous fluids. *Phys. Fluids* **28**, 37–45.

Hu, H. H. & Joseph, D. D. 1989 Lubricated pipelines: stability of core–annular flow. Part 2. *J. Fluid Mech.* **205**, 359–396.

Hyman, J. & Nicolaenko, B. 1986 The Kuramoto–Sivashinsky equation: a bridge between PDE's and dynamical systems. *Physica* D. **18**, 113–126.

Hyman, J., Nicolaenko, B. & Zaleski, S. 1986 Order and complexity in Kuramoto–Sivashinsky model of weakly turbulent interfaces. *Physica* D. **23**, 265–292.

Johnson, M., Kamm, R. D., Ho, L. W., Schapiro, A. & Pedley, T. J. 1991 The nonlinear growth of surface-tension-driven instabilities of a thin annular film. *J. Fluid Mech.* **233**, 141–156.

Kalliadasis, S. & Chang, H.-C. 1994 Drop formation during coating of vertical fibres. *J. Fluid Mech.* **261**, 135–168.

Kamm, R. D. & Schroter, R. C. 1989 Is airway closure caused by a liquid film instability? *Resp. Physiol.* **75**, 141–156.

Kang, F. & Chen, K. 1995 Gravity-driven two-layer flow down a slightly wavy periodic inclined at low Reynolds number. *Intl J. Multiphase Flow* **21**, 501–513.

Kawahara, T. 1983 Formation of saturated solitons in a nonlinear dispersive system with instability and disipation. *Phys. Rev. Lett.* **51**, 381–383.

Kawahara, T. & Toh, S. 1988 Nonlinear dispersive periodic waves in the presence of instability and damping. *Phys. Fluids* **28**, 1636–1638.

Kerchman, V. & Frenkel, A. L. 1994 Interactions of coherent structures in a film flow: simulations of a highly nonlinear evolution equation. *Theor. Comput. Fluid Dyn.* **6**, 235–254.

Kerchman, V. 1995 Strong nonlinear interfacial dynamics in core–annular flows. *J. Fluid Mech.* **290**, 131–166.

Otis, D. R., Jr, Johnson, M., Pedley, T. J. & Kamm, R. D. 1993 Role of pulmonary surfactant in airway closure: a computational study. *J. Appl. Physiol.* **75**, 1323–1333.

Papageorgiou, D. T., Maldarelli, C. & Rumschitzki, D. S. 1990 Nonlinear interfacial stability of core–annular film flows. *Phys. Fluids* A **2**, 340–352.

Papageorgiou, D. T. & Smyrlis, Y. 1991 The route to chaos for the Kuramoto–Sivashinsky equation. *Theor. Comput. Fluid Dyn.* **3**, 15–42.

Pozrikidis, C. 1988 The flow of a liquid film along a periodic wall. *J. Fluid Mech.* **188**, 275–300.

Preziosi, K., Chen, K. & Joseph, D. D. 1989 Lubricated pipelines: stability of flow. *J. Fluid Mech.* **201**, 323–356.

Ransohoff, T. C., Gauglitz, P. A. & Radke, C. J. 1987 Snap-off of gas bubbles in smoothly constricted noncircular capillaries. *AIChE J.* **33**, 753–765.

Ratulowski, J. & Chang, H. C. 1989 In snap-off at strong constrictions: effect of pore geometry. In *Surface-Based Mobility Control: Progress in Miscible Flood Enhanced Oil Recovery* (ed. D. Smith). ACS Symposium Series, vol. 33, pp. 282–314. Hemisphere.

Sivashinsky, G. I. & Michelson, D. M. 1980 On irregular wavy flow of a liquid film down a vertical plane. *Prog. Theor. Phys.* **63**, 2112–2114.

Slattery, J. C. 1974 Interfacial effects in the entrapment and displacement of residual oil. *AIChE J.* **20**, 1145–1154.

Smyrlis, Y. & Papageorgiou, D. T. 1990 Computational study of chaotic and ordered solutions of the Kuramoto–Sivashinsky equation. ICASE Rep.

Tougou, H. 1978 Long waves on a film flow of a viscous fluid down an inclined uneven wall. *J. Phys. Soc. Japan.* **44**, 1014–1019.

Wang, Y. C. 1981 Liquid film flowing slowly down a wavy incline. *AIChE. J.* **27**, 207–212.

Wei, H. H. & Rumschitzki, D. S. 2000 The linear stability of a core–annular flow in a corrugated tube. *IUTAM Symposium on Nonlinear Wave Behavior in Multi-Phase Flow* (ed. H.-C. Chang). Kluwer, Doderecht.

Wei, H. H. & Rumschitzki, D. S. 2002 The linear stability of a core–annular flow in a corrugated tube. *J. Fluid Mech.* **466**, 113–147.